Programmed Cell Death-4 Deficiency Prevents Diet-Induced Obesity, Adipose Tissue Inflammation, and Insulin Resistance

Qun Wang,[1] Zhaojing Dong,[1] Xianglan Liu,[1] Xingguo Song,[1] Qiang Song,[2] Qianwen Shang,[1] Yang Jiang,[1] Chun Guo,[1] and Lining Zhang[1]

Programmed cell death-4 (PDCD4), a selective protein translation inhibitor, has shown proinflammatory effect in some inflammatory diseases, but its roles in obesity remain unestablished. This study aims to investigate the effects of PDCD4 on obesity, inflammation, and insulin resistance. Surprisingly, high-fat diet (HFD)-fed PDCD4-deficient ($PDCD4^{-/-}$) mice exhibited an absolutely lean phenotype together with improved insulin sensitivity. Compared with wild-type obese mice, HFD-fed $PDCD4^{-/-}$ mice showed higher energy expenditure, lower epididymal fat weight, and reduced macrophage infiltration inflammatory cytokine secretion in white adipose tissue (WAT). Alleviated hepatic steatosis along with decreased plasma levels of triglyceride and cholesterol was also observed in these mice. Importantly, PDCD4 appeared to disturb lipid metabolism via inhibiting the expression of liver X receptor (LXR)-α, a master modulator of lipid homeostasis, which was elevated in HFD-fed $PDCD4^{-/-}$ mice accompanied by upregulation of its target genes and relieved endoplasmic reticulum stress in WAT. These data demonstrate that PDCD4 deficiency protects mice against diet-induced obesity, WAT inflammation, and insulin resistance through restoring the expression of LXR-α, thereby proposing PDCD4 as a potential target for treating obesity-associated diseases. ***Diabetes*** **62:4132–4143, 2013**

Obesity is an important independent risk factor for type 2 diabetes, cardiovascular diseases, and many other diseases, including cancer (1–3). Although the underlying mechanism is not fully known, chronic inflammation has been acknowledged as a critical link between obesity and numerous pathologies. Adipose tissue inflammation, characterized by infiltration, activation of inflammatory cells like macrophage and T cells, as well as increased secretion of proinflammatory cytokines and chemokines, including interleukin (IL)-6, IL-8, tumor necrosis factor (TNF)-α, and monocyte chemoattractant protein-1, contributes to low-grade systemic inflammation, insulin resistance, and metabolic disorders, which are referred as the "common soil" for diseases mentioned above (3–7). Therefore, genes or molecules that could control obesity or inflammation will become the promising therapeutic targets for obesity-associated diseases.

Programmed cell death-4 (PDCD4), initially identified as an upregulated gene during apoptosis, is expressed ubiquitously in normal tissues, with highest levels in the liver (8–10). It has been well documented that PDCD4 acts as a regulator of gene expression through influencing translation and transcription. PDCD4 selectively inhibits cap-dependent translation through binding to RNA helicase eukaryotic translation initiation factor (eIF)-4A with its MA-3 domains, which is highly homologous to eIF-4G. Through its inhibitory role in protein translation, PDCD4 suppresses tumor proliferation, invasion, and metastasis and has been considered as a tumor suppressor gene. Loss or reduced expression of PDCD4 has been found in many types of primary tumors (9–15). More recently, emerging evidence has implicated the involvement of PDCD4 in some inflammatory diseases. PDCD4 deficiency in mice not only resists the development of experimental autoimmune encephalomyelitis and type 1 diabetes, but also negatively regulates lipopolysaccharide-induced lethal inflammation (16,17). These data indicate the proinflammatory effects of PDCD4 under certain pathological conditions, while in obesity or obesity-associated inflammation, the roles of PDCD4 and its potential target genes remain unestablished.

Liver X receptor (LXR)-α, a member of the nuclear receptor families, is abundantly expressed in liver, intestine, kidney, spleen, and adipose tissue and functions as a transcription regulator of a series of target genes (18–20). LXR-α promotes lipid homeostasis for its crucial position in cholesterol and fatty acid (FA) metabolism. LXR-α mediates reverse cholesterol transport (RCT), the process of cholesterol trafficking from the peripheral tissues to the liver for excretion and metabolism, by upregulating ATP-binding cassette (ABC) transporters A1 and G1. It also acts as a master regulator in de novo FA synthesis through directly or indirectly regulating lipogenic genes, including sterol regulatory element-binding protein (SREBP)-1c, acetyl-CoA carboxylase, fatty acid synthase (FAS), and stearoyl-CoA desaturase (SCD) 1 (20–23). Additionally, the process of de novo FA synthesis and RCT mediated by LXR-α has been shown to be involved in the maintenance of endoplasmic reticulum (ER) homeostasis, which, in turn, influences obesity and inflammation on different levels (24–27).

In the current study, we demonstrate that PDCD4 deficiency attenuates diet-induced obesity, obesity-associated inflammation, and insulin resistance, accompanied by alleviated hepatic steatosis in mice. These beneficial effects caused by PDCD4 deficiency may result from the derepression of LXR-α in white adipose tissues (WATs) and brown adipose tissues (BATs), which maintain lipid homeostasis and ER balance and increase energy expenditure, thus

From the [1]Department of Immunology, Shandong University School of Medicine, Jinan, Shangdong, China; and the [2]Department of Radiology, Shandong Chest Hospital, Jinan, Shangdong, China.

Corresponding authors: Qun Wang, wangqun@sdu.edu.cn, and Lining Zhang, zhanglining@sdu.edu.cn.

Received 25 January 2013 and accepted 26 August 2013.

DOI: 10.2337/db13-0097

This article contains Supplementary Data online at http://diabetes.diabetesjournals.org/lookup/suppl/doi:10.2337/db13-0097/-/DC1.

linking the modulation of PDCD4 to LXR function and proposing PDCD4 as a potential therapeutic target for obesity-associated diseases.

RESEARCH DESIGN AND METHODS

Animals and diets. PDCD4-deficient ($PDCD4^{-/-}$) mice generated on C57BL/6 background were provided by Youhai H. Chen, University of Pennsylvania School of Medicine. Obesity was induced in male $PDCD4^{-/-}$ or wild-type (WT) mice by feeding a high-fat diet (HFD) containing 15% w/w fat and 0.25% cholesterol beginning at the age of 8 weeks; mice on a normal diet (ND) were used as lean controls (28,29). Body weight was recorded every 2 weeks, and daily food intake was calculated during the last 8 weeks of diet interventions. After 24 weeks, mice were killed under anesthesia. Serum, epididymal fat pads, BAT, and liver were collected. All animal studies were approved by the Animal Care and Utilization Committee of Shandong University. All experimental procedures were in accordance with institutional guidelines.

Metabolic parameters measurements. Plasma triglyceride (TG) and total cholesterol (TC) were detected with an automated chemically modified technique (Roche Modular DPP System, Roche, Switzerland). Fasting plasma levels of glucose and insulin were measured with OneTouch Ultra in-vitro diagnosticum (LifeScan, Milpitas, CA) and with mouse insulin ELISA kit (RD, Wuhan, China), respectively, then the homeostasis model assessment of insulin resistance (HOMA-IR) was calculated. Glucose tolerance test (GTT) was performed in mice with an overnight fast. Blood glucose was measured before and at the indicated time after an intraperitoneal injection of D-glucose (2 g/kg body weight; Sigma-Aldrich, St. Louis, MO). Insulin tolerance test (ITT) was performed in mice with free access to food and water. Blood glucose was measured before and at the indicated time after an intraperitoneal injection of human insulin (0.75 units/kg body weight; Wanbang, Xuzhou, China).

Energy expenditure and locomotor activity measurements. Energy expenditure of an individual mouse was measured for 48 h using metabolic cages (TSE systems, Bad Homburg, Germany). Respiratory exchange ratio was calculated as VCO_2/VO_2, which was normalized to body weight. The locomotor activity was recorded as travel distances every 10 min using video-tracking system (SMART, San Diego, CA).

Histology and immunohistochemistry. Mice liver and adipose tissues were fixed in 4% paraformaldehyde (Sigma-Aldrich), embedded in paraffin, and sectioned. The sections were stained with hematoxylin and eosin (HE) using standard protocol. For adipose tissue section, the average diameter of adipocytes was measured using Image-Pro Plus 6.0, the macrophage infiltration was determined by immunohistochemical staining using rat antibody against mouse CD68 (Bioss, Beijing, China).

Hepatic triglyceride qualification. A piece of liver tissue was homogenized in Folch reagent, and total lipid was extracted from liver homogenate and dried. The lipid extract dissolved in isopropanol and TG contents were measured with a triglyceride test kit (BHKT Clinical Reagent, Beijing, China). Hepatic TG contents were normalized to liver wet weight.

Adipose tissue explants culture. Epididymal adipose tissues from mice were collected and cut into small pieces. The minced adipose tissue explants were cultured in Dulbecco's modified Eagle's medium (Gibco, Invitrogen, Carlsbad, CA) supplemented with 10% FCS, 1% streptomycin/penicillin at 37°C in a humidified atmosphere of 5% CO_2; 1 ml Dulbecco's modified Eagle's medium was added per 0.3 g of adipose tissue explants. After 24 h, the supernatants were collected for inflammation assay.

Cytometric bead array immunoassay. Serum from individual mice and supernatants from cultured adipose explants were assayed for inflammatory markers using cytometric bead array mouse inflammation kit (BD Biosciences, Franklin Lakes, NJ) as per the manufacturer's recommendations. Data were collected with Cytomics FC500 (Beckman Coulter, Brea, CA).

Quantitative reverse transcription PCR. Total RNA was isolated using Trizol reagent (Invitrogen). Quantitative reverse transcription PCR was performed to examine mRNA levels of target molecules relative to 18S rRNA. Primers used are listed in Supplementary Table 1.

Western-blot assay. Tissues or cells were lysed in SDS buffer in the presence of protease inhibitor and phosphatase inhibitor. Equal amounts of protein were separated on SDS-PAGE and blotted onto polyvinylidene fluoride membranes (Millipore, Billerica, MA). After blocking with 1% bovine serum albumin in Tris-buffered saline with Tween (containing 0.1% Tween-20) for 1 h, membranes were probed overnight at 4°C with antibodies against mouse phospho(p)-protein kinase-like endoplasmic reticulum kinase (Perk), p-eIF2α, p-c-Jun N-terminal kinase (JNK), SCD1 (Cell Signaling Technology, Beverly, MA), X-box binding protein-1, SREBP-1c, LXR-α (Abcam, Cambridge, MA), FAS, uncoupling protein (UCP)-1 (Proteintech Group, Chicago, IL), and peroxisome proliferator-activated receptor-γ coactivator (PGC)-1α (Sigma-Aldrich), respectively, followed by peroxidase-labeled secondary antibodies for 1 h at room temperature. After washing, signals were visualized by SuperSignal West Pico Chemiluminescent Substrate (Pierce Biotechnology, Rockford, IL).

RNA-binding protein immunoprecipitation. RNA-binding protein immunoprecipitation (RIP) experiments were performed using a Magna RIP kit (Millipore) according to the manufacturer's procedures. Briefly, cells were collected and lysed in RIP lysis buffer, 10% supernatants were saved as the input sample, and the remaining supernatants were used for immunoprecipitation at 4°C overnight with rabbit antibody against mouse PDCD4 (Cell Signaling Technology), which was prebound to magnetic beads. Normal rabbit IgG served as negative control. The immunoprecipitates were digested in proteinase K buffer at 55°C for 30 min. After elution from the beads, RNA was extracted and purified. cDNA synthesis and quantitative reverse transcription PCR were performed to detect LXR-α mRNA.

Statistical analysis. GraphPad Prism 5 was used for statistical analyses. ANOVA or Student t tests were performed to determine significance. Values are presented as mean ± SEM. Differences were considered significant when $P < 0.05$.

RESULTS

PDCD4 deficiency inhibits adiposity and reduces epididymal fat weight in HFD-fed mice. To investigate the role of PDCD4 in obesity, $PDCD4^{-/-}$ and WT mice were fed a HFD for 24 weeks, using littermates fed a ND as lean controls. At the end of the study, HFD-fed WT mice had an obviously increased body weight compared with lean controls, whereas HFD-fed $PDCD4^{-/-}$ mice, similar to ND-fed mice, failed to gain body weight from 12th to 24th week (Fig. 1*A*, *B*, and *D*). The lean phenotype of HFD-fed $PDCD4^{-/-}$ mice was independent on diet intake, for no alteration of food intake was observed (Fig. 1*C*). Furthermore, the epididymal fat weight and the ratio of epididymal fat weight to body weight were also markedly decreased in HFD-fed $PDCD4^{-/-}$ mice compared with those in HFD-fed WT mice, while no difference was observed when compared with those in ND-fed mice (Fig. 1*D–F*). These results indicate PDCD4 deficiency causes a resistance to HFD-induced obesity, primarily due to the decrease of epididymal fat weight.

PDCD4 deficiency improves metabolic homeostasis in HFD-fed mice. At the end of the study, plasma TG and TC levels in HFD-fed $PDCD4^{-/-}$ mice were markedly lower than those in WT obese mice, and fasting plasma glucose levels had a decreasing trend, although no significant difference was observed during HFD intervention (Fig. 2*A–C*). Importantly, HFD-fed $PDCD4^{-/-}$ mice had much lower HOMA-IR and plasma levels of insulin than WT obese mice (Fig. 2*D–E*), showing more glucose tolerance and insulin sensitivity, as evidenced by decreased glucose levels 60 min after glucose injection (until the end of GTT) and 15 min after insulin injection. In particular, HFD-fed $PDCD4^{-/-}$ mice showed obviously lower area under the curve values during ITT (Fig. 2*F–H*).

PDCD4 deficiency increases energy expenditure in HFD-fed mice. To determine whether the lean phenotype of HFD-fed $PDCD4^{-/-}$ mice was due to increased energy expenditure, we performed energy expenditure in WT and $PDCD4^{-/-}$ mice fed a ND or HFD. As expected, no significant difference was observed between ND-fed WT and $PDCD4^{-/-}$ mice (Fig. 3*A*). Compared with WT obese mice, HFD-fed $PDCD4^{-/-}$ mice showed much higher energy expenditures, especially in dark phases (Fig. 3*B* and *C*), which seemed to be independent of respiratory exchange ratio and locomotor activity since no significant alterations were found in both of them between HFD-fed $PDCD4^{-/-}$ and WT mice (Fig. 3*D–F*). Unexpectedly, an obvious upregulation of PGC-1α but not UCP-1 was present in BAT

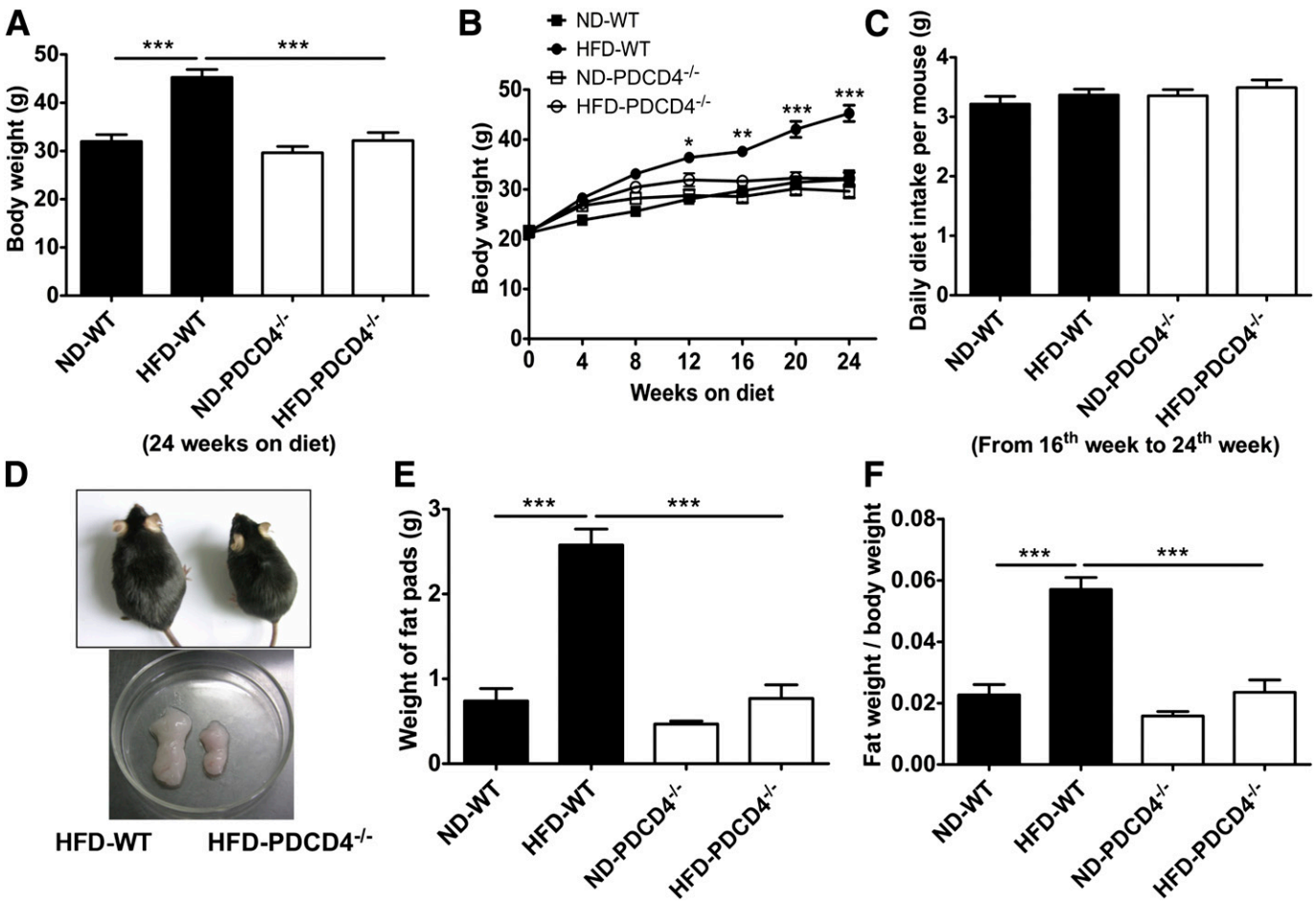

FIG. 1. Effects of PDCD4 deficiency on adiposity in HFD-fed mice. WT (n = 10) and PDCD4$^{-/-}$ (n = 6) mice were fed a ND or HFD for 24 weeks. Body weight change, diet intake, and weight of epididymal fat pads were assessed. (*A*) The body weight on 24-week diet, (*B*) body weight change, and (*C*) daily diet intake of WT and PDCD4$^{-/-}$ mice. (*D*) The gross morphology of WT and PDCD4$^{-/-}$ mice fed a HFD and epididymal fat pads from these mice. (*E*) The weight of epididymal fat pads, and (*F*) the ratio of fat weight to body weight of WT and PDCD4$^{-/-}$ mice. Results are presented as mean ± SEM. Data are representative of three or more independent experiments. *P < 0.05, **P < 0.01, ***P < 0.001.

(Fig. 3*G* and *H*), which might partially account for the increased energy expenditure in HFD-fed PDCD4$^{-/-}$ mice.

PDCD4 deficiency reduces adipocyte hypertrophy in HFD-fed mice. Next, adipocyte size and related gene expression in epididymal adipose tissues were examined. Unlike HFD-fed WT mice that displayed apparent adipocyte hypertrophy, HFD-fed PDCD4$^{-/-}$ mice, similar to the lean mice, maintained a relatively normal adipocyte size (Fig. 4*A* and *B*). Accordingly, PDCD4 deficiency led to a decrease in mRNA levels of leptin, which was highly correlated with the visceral fat mass, and increases in mRNA levels of adiponectin, peroxisome proliferator–activated receptor (PPAR)-γ, and CCAAT/enhancer binding protein (c/EBP) α related to adipocyte differentiation during HFD feeding, which were comparable to the mRNA levels of ND-fed mice. Additionally, no correlation was found between adiponectin mRNA level and visceral fat mass (Fig. 4*C–H*). These data indicate PDCD4 deficiency suppresses the adipocyte hypertrophy but maintains the normal adipocyte differentiation program in HFD-fed mice.

PDCD4 deficiency attenuates WAT inflammation in HFD-fed mice. Since the visceral fat accumulation in obese mice is usually accompanied by WAT inflammation and low levels of systemic inflammation, we further detected WAT and serum inflammatory status in HFD-fed PDCD4$^{-/-}$ mice. The percentage of CD68^{+} macrophage in epididymal adipose tissues from HFD-fed PDCD4$^{-/-}$ mice was much lower than that from WT obese mice (Fig. 5*A* and *B*), indicating reduced macrophage infiltration in HFD-fed PDCD4$^{-/-}$ mice. Consistently, proinflammatory cytokines IL-6 and TNF-α secreted by the cultured adipose explants from HFD-fed PDCD4$^{-/-}$ mice also markedly decreased (Fig. 5*C–I*). Furthermore, serum inflammatory cytokine, including IL-6, TNF-α, interferon-γ, IL-12, and chemokine monocyte chemoattractant protein-1, also showed decreasing trends in HFD-fed PDCD4$^{-/-}$ mice, although no significant differences were observed compared with WT obese mice (Supplementary Fig. 1). These data demonstrate that PDCD4 deficiency attenuates WAT inflammation in HFD-fed mice.

PDCD4 deficiency alleviates hepatic steatosis in HFD-fed mice. Given that HFD-induced obese mice display not only increased fat accumulation, but also hepatic steatosis, liver tissues from PDCD4$^{-/-}$ or WT mice were collected for steatosis and TG analysis. Liver tissues from HFD-fed PDCD4$^{-/-}$ mice were darker and lighter than those from WT obese mice, although the ratio of liver weight to body weight had no significant difference (Fig. 6*A–C*). As expected, HFD-fed WT mice had severe fatty liver with numerous lipid droplets in liver sections, while HFD-fed PDCD4$^{-/-}$ mice showed alleviated hepatic steatosis, as evidenced by few lipid droplets in tissue

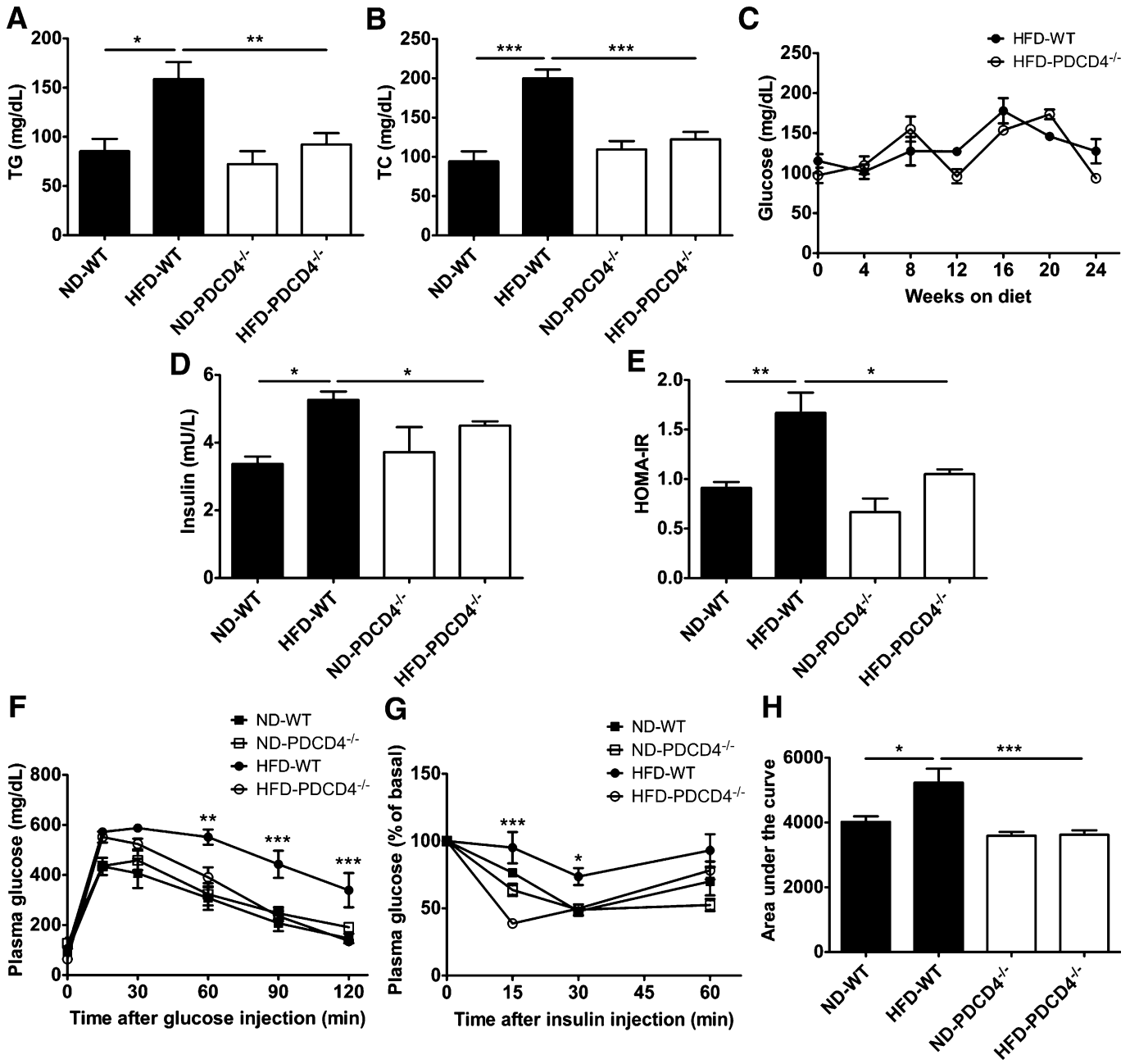

FIG. 2. PDCD4 deficiency improves metabolic homeostasis in HFD-fed mice. WT and PDCD4$^{-/-}$ mice were fed a ND or HFD for 24 weeks. Metabolic parameters were analyzed. (*A*) TG and (*B*) TC of WT (n = 18–22) and PDCD4$^{-/-}$ (n = 18–19) mice. (*C*) Fasting blood glucose during the diet intervention ($n \geq 3$ mice/group). (*D*) Fasting plasma insulin and (*E*) HOMA-IR of WT and PDCD4$^{-/-}$ mice (n = 4–5 mice/group). (*F*) GTT (n = 5–7 mice/group), (*G*) ITT (n = 4–7 mice/group), and (*H*) area under the curve in ITT. Data are presented as mean ± SEM. *$P < 0.05$, **$P < 0.01$, ***$P < 0.001$, HFD-fed WT vs. HFD-fed PDCD4$^{-/-}$ mice.

sections and much lower hepatic TG contents than WT obese mice (Fig. 6*D* and *E*). Additionally, PDCD4 deficiency also led to substantially decreased mRNA and protein levels of SREBP-1c, FAS, and SCD1 in the liver from HFD-fed mice (Fig. 6*F*–*I*), indicating PDCD4 deficiency ameliorates hepatic steatosis in HFD-fed mice probably through inhibiting hepatic lipogenesis.

PDCD4 deficiency restores the expression of LXR-α in WAT from HFD-fed mice. Considering the pivotal role of LXR-α in maintaining lipid homeostasis and ER balance (26,27,30,31), we further examined the expression of LXR-α and its target genes, as well as ER stress markers in WAT from PDCD4$^{-/-}$ or WT mice. As shown in Fig. 7*A* and *B*, only LXR-α protein, but not its mRNA, was repressed in WT obese mice compared with lean controls; however, both of them substantially restored or elevated in HFD-fed PDCD4$^{-/-}$ mice accompanied by upregulation of LXR-α target genes such as SREBP-1c, FAS, SCD1, ABCA1, and ABCG1 (Fig. 7*C*–*H*). Consistent with previous reports, WT obese mice had enhanced ER stress markers in WAT compared with lean controls (25,32–34), while HFD-fed PDCD4$^{-/-}$ mice showed markedly attenuated ER stress markers, including p-Perk, p-eIF2α, and spliced X-box binding protein-1, and the downstream inflammatory pathway signal JNK1/2 also reduced significantly (Fig. 7*I*). These findings indicate that PDCD4 deficiency could

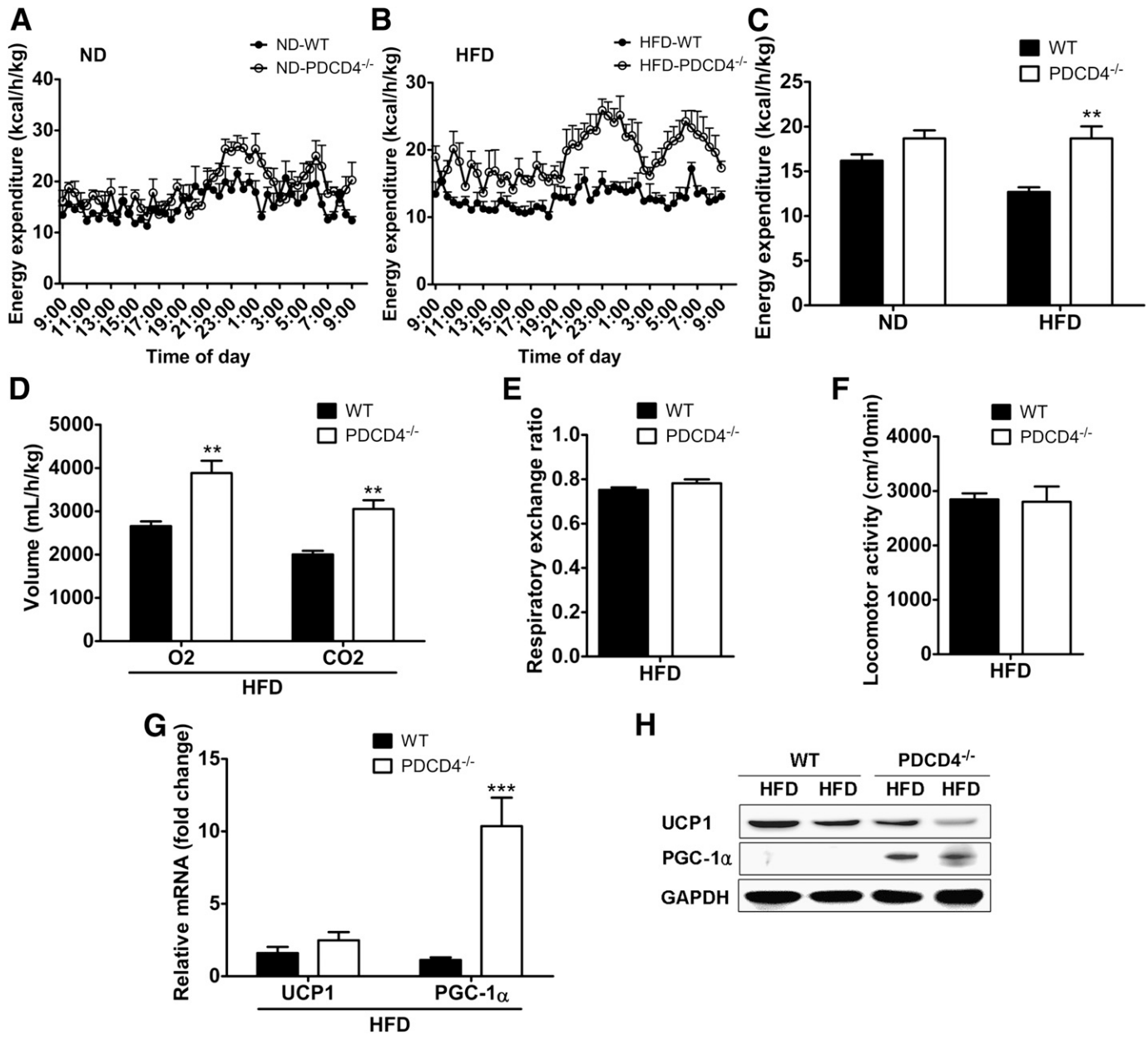

FIG. 3. PDCD4 deficiency increases energy expenditure in HFD-fed mice. Metabolic cage studies were performed in WT and PDCD4$^{-/-}$ mice fed a ND or HFD for 24 weeks. Energy expenditure of (*A*) ND-fed or (*B*) HFD-fed mice and (*C*) the statistic data ($n \geq 3$ mice/group). (*D*) O2 consumption and CO2 production, (*E*) respiratory exchange ratio, and (*F*) locomotor activity ($n = 6$ mice/group) of HFD-fed WT or PDCD4$^{-/-}$ mice. (*G*) mRNA levels and (*H*) representative Western-blot of UCP1 and PGC-1α in BAT from HFD-fed WT or PDCD4$^{-/-}$ mice ($n = 4$/group). Data are presented as mean ± SEM. GADPH, glyceraldehyde-3-phosphate dehydrogenase. **$P < 0.01$, ***$P < 0.001$.

restore the expression of LXR-α in WAT from HFD-fed mice and, in turn, facilitate the maintenance of lipid homeostasis and ER balance. Besides, the elevation of LXR-α in liver and BAT from HFD-fed PDCD4$^{-/-}$ mice was also verified (Supplementary Fig. 2*A*–*C*), indicating LXR-α might be a potential inhibitory target of PDCD4 in HFD-fed mice.

PDCD4 inhibits LXR-α protein expression through binding to its mRNA. To further clarify the regulation of PDCD4 on LXR-α in high-fat circumstances, 3T3-L1 adipocytes and macrophages from PDCD4$^{-/-}$ or WT mice were used to treat oxidized LDL (oxLDL). For oxLDL-treated adipocytes, the LXR-α protein obviously decreased after a transient elevation, and accordingly, the lipid contents reached a higher level (Fig. 8*A* and *B*, Supplementary Fig. 3*A*), indicating oxLDL stimulation could cause the suppression of LXR-α and lipid accumulation in adipocytes. Similar results were observed in oxLDL or palmitate acid (PA)-stimulated WT macrophages. In contrast, for oxLDL or PA-stimulated PDCD4$^{-/-}$ macrophages, the elevation of LXR-α was accompanied by dramatically reduced lipid contents (Fig. 8*C* and *D*, Supplementary Fig. 3*B*), while silencing of LXR-α markedly reversed the lipid contents, which was accompanied by downregulation of LXR-α target genes like ABCG1, SCD1, and FAS (Fig. 8*E*–*G*, Supplementary Fig. 3*C*), thus the lipid removal caused by PDCD4 deficiency was mediated at least partially by the elevation of LXR-α.

It has been recognized PDCD4 inhibits protein translation via direct or indirect binding to the mRNA of

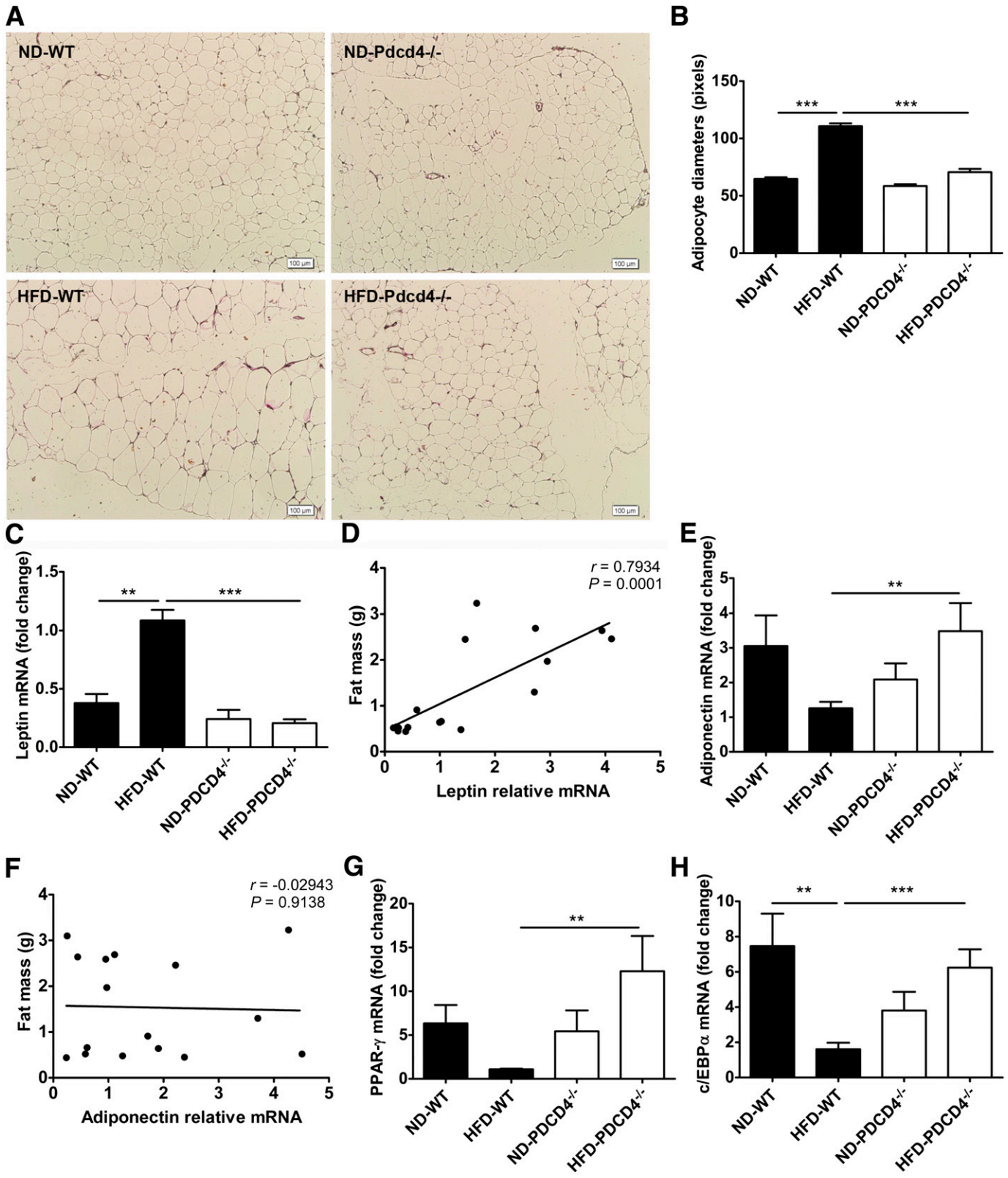

FIG. 4. PDCD4 deficiency reduces adipocyte hypertrophy in HFD-fed mice. WT and PDCD4$^{-/-}$ mice were fed a ND or HFD for 24 weeks. The adipocyte size and mRNA levels of fat-related genes were analyzed. (*A*) Histological analysis (HE staining) on sections of epididymal adipose tissues ($n \geq 3$ mice/condition). Original magnification is 100, scale bar is 100 μm. (*B*) The average diameters of adipocytes in randomly chosen fields were measured and presented as pixels using Image-Pro Plus 6.0. (*C*) Leptin and (*E*) adiponectin mRNA levels in epididymal adipose tissues (n = 5–7 mice/group) and (*D* and *F*) the correlation of mRNA level with epididymal fat mass (n = 18). (*G*) PPAR-γ and (*H*) c/EBPα mRNA levels in epididymal adipose tissues (n = 4–9 mice/group). Data are presented as mean ± SEM. **$P < 0.01$, ***$P < 0.001$.

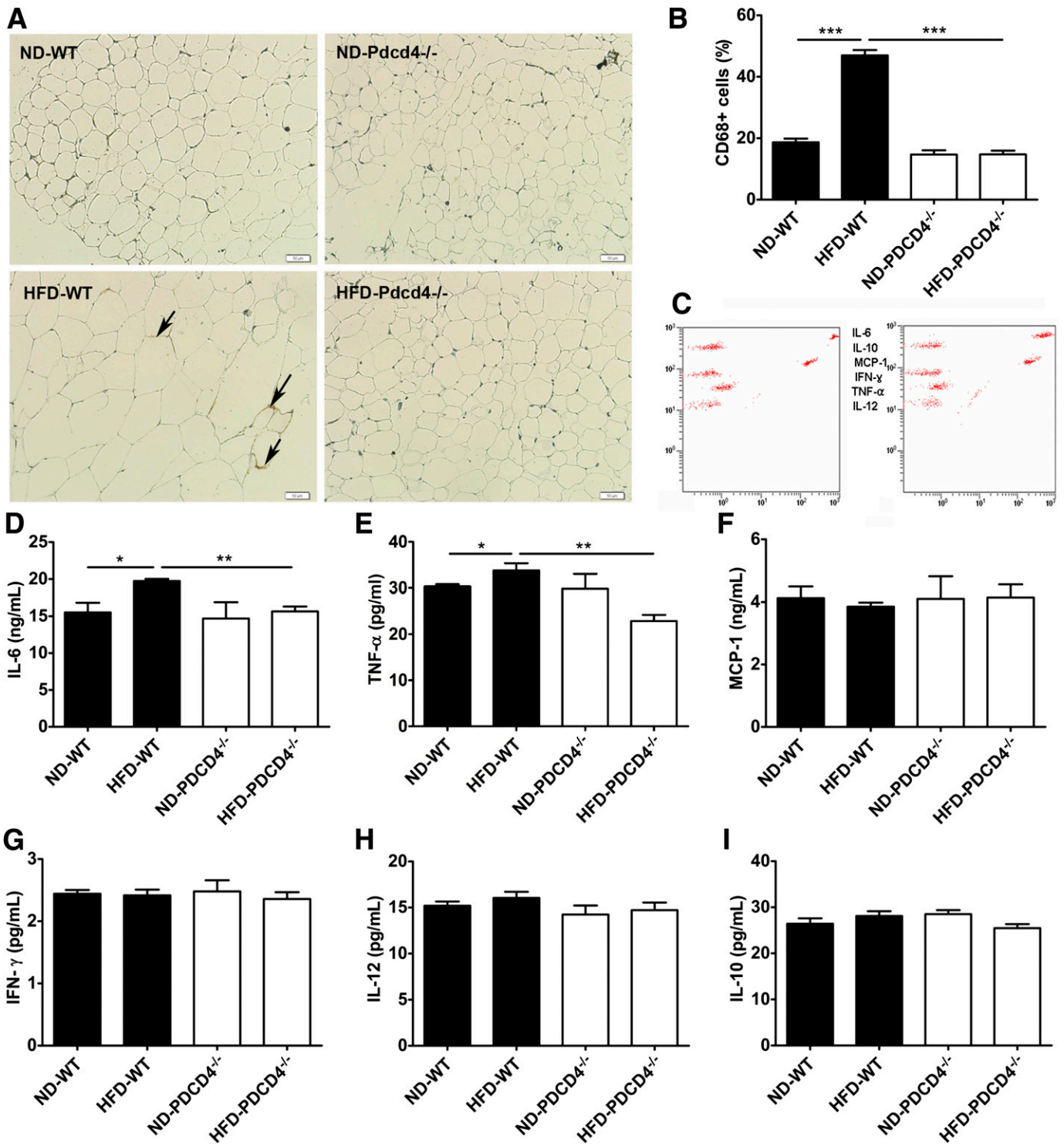

FIG. 5. PDCD4 deficiency attenuates WAT inflammation in HFD-fed mice. WT and PDCD4$^{-/-}$ mice were fed a ND or HFD for 24 weeks. The macrophage infiltration in epididymal adipose tissues and inflammatory cytokine secretion by epididymal adipose tissue explants were detected. (*A*) Immunohistochemical study (CD68 staining) and (*B*) percentage of CD68^{+} macrophages on sections from epididymal adipose tissues ($n \geq 3$ mice/condition); the arrows indicate inflammation. Original magnification is 200, scale bar is 50 μm. (*C*) Representative data of cytometric bead array immunoassay and (*D–I*) statistical data for inflammation detection on supernatants from cultured epididymal adipose tissue explants (n = 4–9 mice/group). Data are presented as mean ± SEM. IFN-γ, interferon-γ; MCP, monocyte chemoattractant protein. *$P < 0.05$, **$P < 0.01$, ***$P < 0.001$.

target gene (9,35,36). To determine whether PDCD4 inhibits LXR-α expression by this mechanism, we performed RIP assay in oxLDL-stimulated WT macrophage using anti-PDCD4 antibody. As shown in Fig. 8*H*, LXR-α mRNA was successfully enriched in the PDCD4-specific immunoprecipitate compared with the control precipitate, thus revealing the binding of PDCD4 with LXR-α mRNA in response to oxLDL stimulation and supporting the idea that PDCD4 inhibits the translation of LXR-α mRNA.

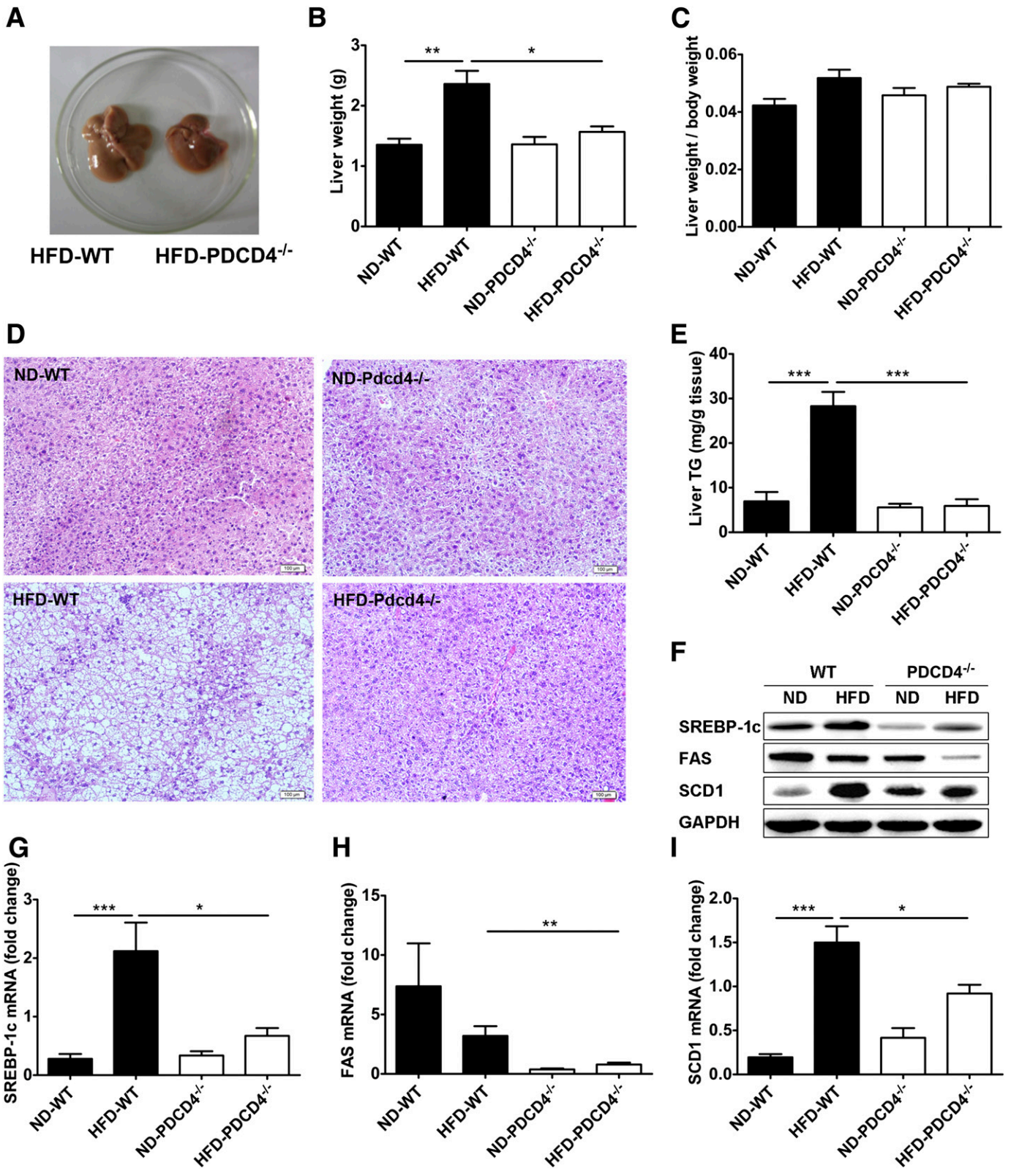

FIG. 6. PDCD4 deficiency alleviates hepatic steatosis in HFD-fed mice. WT and PDCD4$^{-/-}$ mice were fed a ND or HFD for 24 weeks, and livers were collected for histological analysis, hepatic TG quantification, and lipogenic genes analysis. (*A*) The gross morphology of liver, (*B*) liver weight, (*C*) the ratio of liver weight to body weight, (*D*) and histological analysis (HE staining) of liver tissue sections from WT and PDCD4$^{-/-}$ mice ($n \geq 3$ per condition). (*E*) Hepatic TG contents in HFD-fed WT and PDCD4$^{-/-}$ mice (n = 5–8 mice/group). (*F*) Representative Western-blot and mRNA levels of (*G*) SREBP-1c, (*H*) FAS, and (*I*) SCD1 in liver tissues from ND or HFD-fed WT and PDCD4$^{-/-}$ mice (n = 4–9 mice/group). Data are presented as mean ± SEM. GADPH, glyceraldehyde-3-phosphate dehydrogenase. *$P < 0.05$, **$P < 0.01$, ***$P < 0.001$.

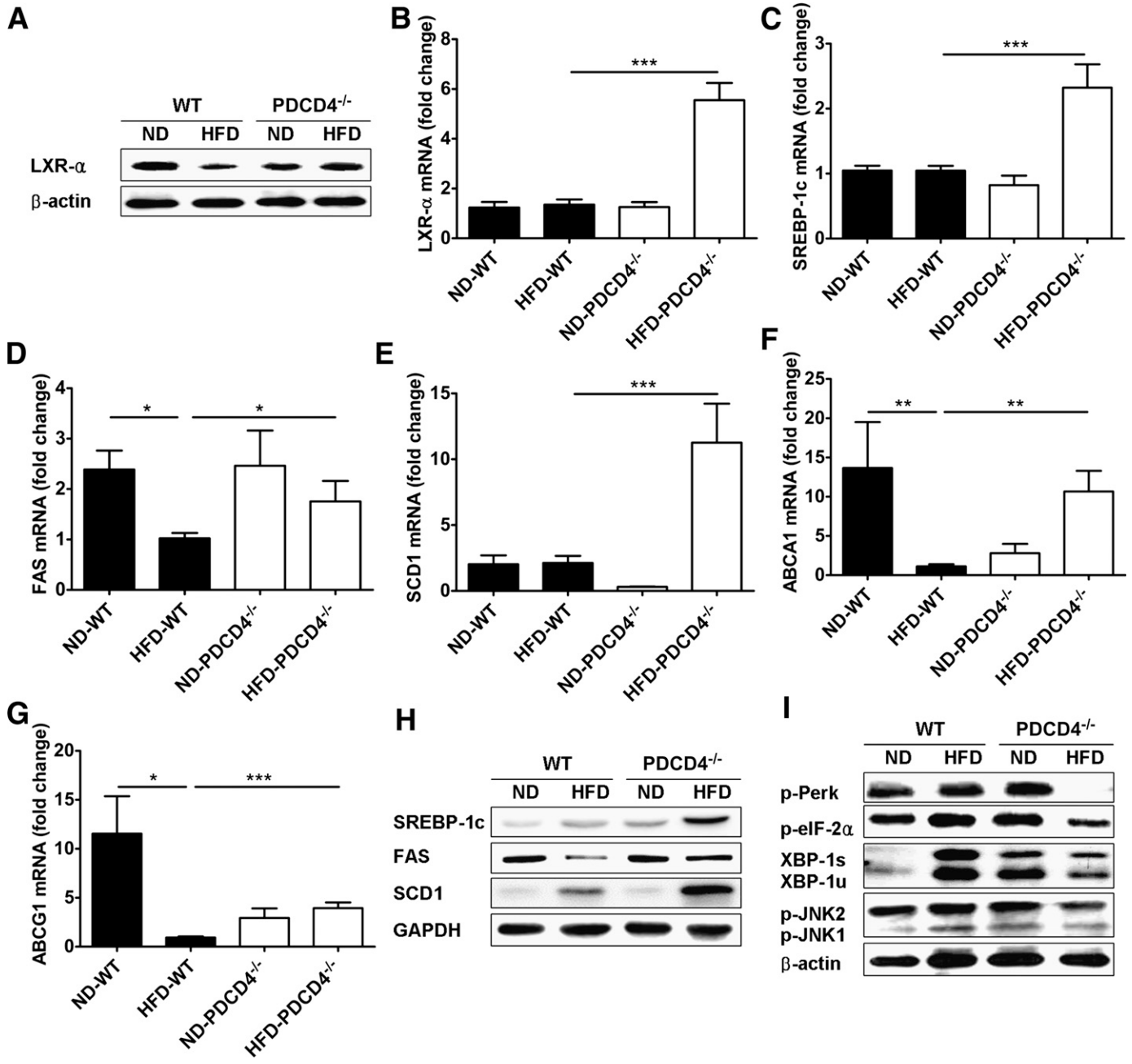

FIG. 7. Effects of PDCD4 deficiency on LXR-α expression and ER homeostasis in WAT. Epididymal adipose tissues were collected from WT and PDCD4$^{-/-}$ mice fed a ND or HFD for 24 weeks. The expression of LXR-α and its target genes, as well as ER stress markers, were examined. (*A*) Representative Western-blot of LXR-α in epididymal adipose tissues (n = 3 mice/condition). (*B*) mRNA levels of LXR-α in epididymal adipose tissues (n = 12 WT mice or 8 PDCD4$^{-/-}$ mice). mRNA levels and (*H*) representative Western-blot of (*C*) SREBP-1c, (*D*) FAS, (*E*) SCD1, (*F*) ABCA1, and (*G*) ABCG1 in epididymal adipose tissues (n = 4–9 mice/group). (*I*) Representative Western-blot of ER stress markers in epididymal adipose tissues (n = 3 mice/condition). Data are presented as mean ± SEM. GADPH, glyceraldehyde-3-phosphate dehydrogenase; XBP, X-box binding protein. *P < 0.05, **P < 0.01, ***P < 0.001.

DISCUSSION

While PDCD4 is well accepted as a tumor suppressor gene, emerging evidence indicates its proinflammatory effects in some pathological conditions. In obesity and associated inflammation, the roles of PDCD4 remain unestablished. In this study, we have shown that PDCD4 deficiency brings multiple beneficial effects in HFD-fed mice, as indicated by alleviated adiposity, WAT inflammation, hepatic steatosis, and improved insulin action.

Through the study of HFD-fed PDCD4$^{-/-}$ mice, we surprisingly found PDCD4 deficiency conferred absolute resistance to HFD-induced obesity in mice. Although there were no alterations in food intake, respiratory exchange ratio, and locomotor activity between HFD-fed PDCD4$^{-/-}$ and WT mice, HFD-fed PDCD4$^{-/-}$ mice still showed increased energy expenditure compared with WT obese mice, indicating PDCD4 deficiency might influence thermogenesis of HFD-fed mice. As expected, dramatic elevation of PGC-1α was found in BAT from HFD-fed PDCD4$^{-/-}$ mice, which could be one important contributor to the antiobesity effects of PDCD4 deficiency.

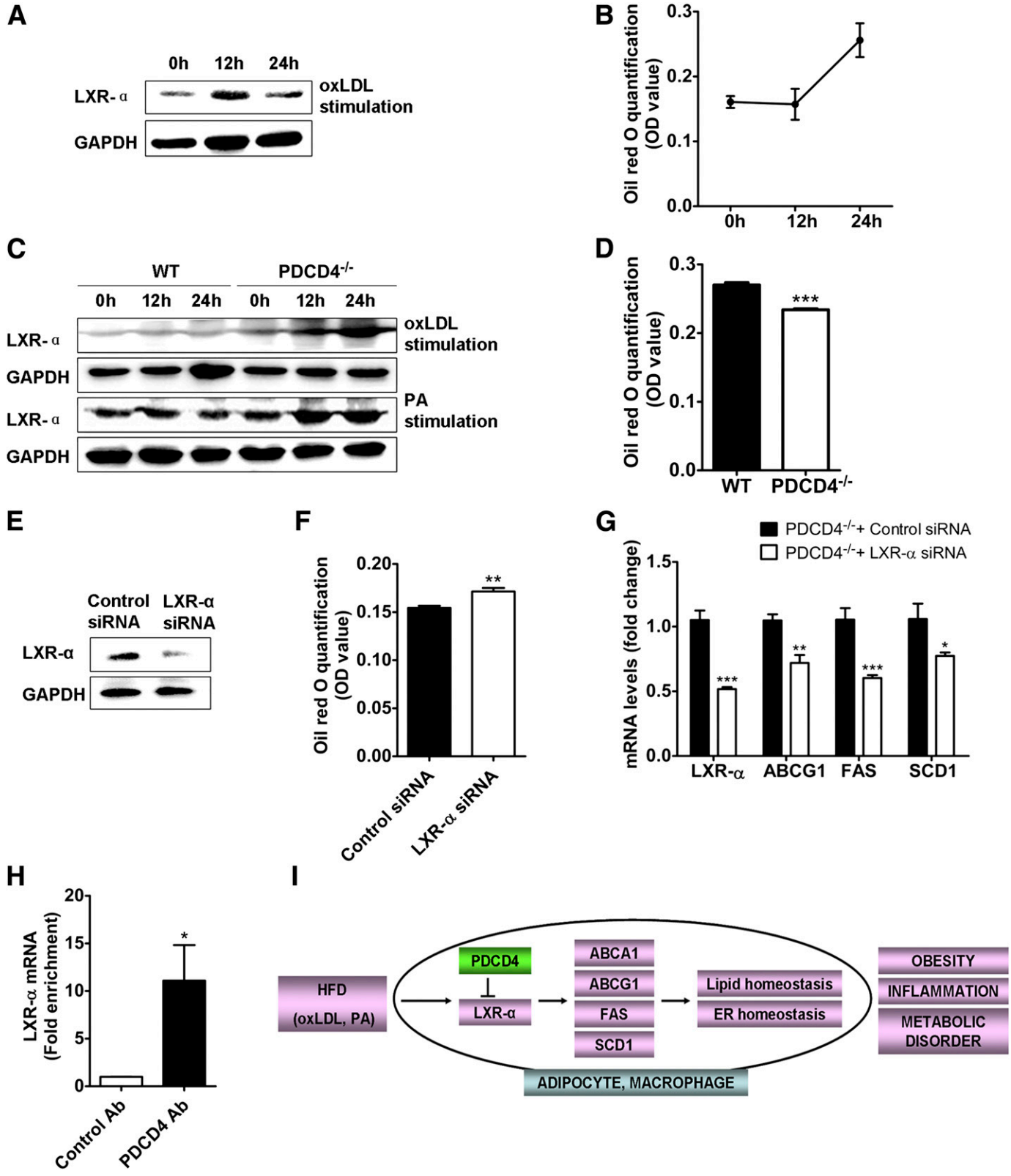

FIG. 8. Role of PDCD4 in LXR-α expression. Representative Western-blot of (*A*) LXR-α and (*B*) lipid quantification in oxLDL (50 μg/mL)-treated 3T3-L1 adipocytes for indicated time. Macrophages from WT or PDCD4$^{-/-}$ mice (n = 3 mice/genotype) were treated with oxLDL (50 μg/mL) or PA (500 μmol/L) for indicated time. (*C*) Representative Western-blot of LXR-α and (*D*) lipid quantification in macrophages treated with oxLDL for 24 h. Macrophages from PDCD4$^{-/-}$ mice (n = 3 mice/genotype) were transfected with control or LXR-α siRNA. After 48 h, the cells were treated with oxLDL (50 μg/mL) for additional 24 h. (*E*) Representative Western-blot of LXR-α, (*F*) lipid quantification, and (*G*) mRNA levels of LXR-α and its downstream genes in PDCD4$^{-/-}$ macrophages. (*H*) Fold enrichment for LXR-α mRNA in RIP assay on oxLDL-treated WT macrophages using PDCD4 antibody. (*I*) A working model showing the role of PDCD4 in diet-induced obesity. In response to HFD, PDCD4 disturbs the homeostasis of lipid metabolism and ER function via selectively inhibiting the upregulation of LXR-α and its target genes, thereby leading to obesity, WAT inflammation, and metabolic disorders. Data are presented as mean ± SEM. Ab, antibody; GADPH, glyceraldehyde-3-phosphate dehydrogenase; OD, optical density; siRNA, small interfering RNA. *P < 0.01, **P < 0.01, ***P < 0.001.

Consistent with the lean phenotype, HFD-fed PDCD4$^{-/-}$ mice showed reduced epididymal fat weight compared with WT obese mice. Notably, the adipocytes in WAT from HFD-fed PDCD4$^{-/-}$ mice exhibit resistance to hypertrophy and impaired differentiation. The adipocyte size was quite normal, as that in ND-fed mice, and the expression of adiponectin, PPAR-γ, and c/EBPα also reversed to a normal or higher level, indicating PDCD4 deficiency is helpful to maintain the lipid homeostasis of WAT when the mice suffered from HFD. The lean phenotype itself contributed to the alleviated WAT inflammation and improved insulin actions in HFD-fed PDCD4$^{-/-}$ mice. Another major contributor could be ER homeostasis, which has been reported to provide protection against obesity, inflammation, and insulin resistance on different levels (26,30,31,37,38). Compared with WT obese mice, HFD-fed PDCD4$^{-/-}$ mice showed significantly attenuated ER stress markers in WAT together with reduced activation of proinflammatory JNK pathway. Accordingly, the macrophage infiltration was reduced in WAT and TNF-α, IL-6 secretion reduced markedly, and the insulin action substantially improved, as indicated by increased glucose tolerance and insulin sensitivity. These data suggest that ER homeostasis caused by PDCD4 deficiency may contribute to the reduced WAT inflammation and insulin resistance via inhibiting JNK pathway.

Another desirable effect of PDCD4 deficiency is alleviated hepatic steatosis in HFD-fed mice, accompanied by decreased plasma TG and TC levels. The hepatic lipogenesis in HFD-fed PDCD4$^{-/-}$ mice was substantially inhibited, as reflected by decreased expression of lipogenous gene SREBP-1c. This action resulted in decreased hepatic TG contents and attenuated oxidative stress in the liver (Supplementary Fig. 4) and further led to improved insulin sensitivity. With respect to the reasons for reduced hepatic lipogenesis in HFD-fed PDCD4$^{-/-}$ mice, many factors like adiponectin, FA, and LXR-α could produce multiple effects via regulating SREBP-1c (39,40). However, in this study, a very likely contributor might be decreased insulin levels, which is a consequence of improved insulin action in HFD-fed PDCD4$^{-/-}$ mice since insulin has been recognized as a primary stimulator to active hepatic lipogenesis through selectively inducing SREBP-1c even in insulin-resistant obese mice (41,42).

Interestingly, we have shown PDCD4 deficiency causes the restoration or elevation of LXR-α in both the adipose and the liver of HFD-fed mice, as well as in PA or oxLDL-simulated macrophages, which may contribute to the beneficial effects due to their coordinate role in metabolic effects. First, the restoration of LXR-α in WAT or macrophages facilitates lipid homeostasis and ER balance in multiple ways. LXR-α not only drives RCT to remove cholesterol, but also increases lipolysis and FA β-oxidation to prevent the cells from lipid overload (23,43). Consistent with the study from Erbay et al. (26), LXR-α and downstream SCD1 could induce resistance to ER stress via efficient desaturation of FA, thus maintaining the ER homeostasis in WAT or macrophages. Second, the elevation of LXR-α in BAT is involved in the regulation of energy expenditure via upregulating PGC-1α. This viewpoint is supported by our observation showing concomitant upregulation of LXR-α and PGC-1α in BAT from HFD-fed PDCD4$^{-/-}$ mice and a recent report showing that the activation of LXR-α produces antiobesity effect in HFD-fed obese mice partially through elevated PGC-1α mRNA in BAT (44). Third, the restoration of LXR-α in the liver may also contribute to the alleviated fatty liver despite its lipogenous effects. This possibility is supported by a recent study demonstrating LXR-α increases long-chain acyl-CoA synthetase 3 expression in hamster liver, which could direct hepatic FA entry into the catabolic pathway to reduce TG accumulation in liver tissue (45). Our observations are somewhat different from several studies from LXR$^{-/-}$ mice (46); the reasons for this discrepancy may be different mouse models and experiment designs. Moreover, the expression of gluconeogenesis-related genes phosphoenolpyruvate carboxykinase, glucose-6-phosphatase in the liver, and glucose-uptake-related gene insulin-sensitive glucose transporter 4 in adipose tissues showed no significant differences between HFD-fed PDCD4$^{-/-}$ and WT mice (Supplementary Fig. 5*A–C*), indicating the regulation of LXR-α in HFD-fed PDCD4$^{-/-}$ mice may have relatively minor effects on glucose homeostasis; otherwise, the beneficial effects are sheltered by other regulatory processes. It is worth noting we cannot exclude the contribution of other unidentified targets of PDCD4, which need to be further investigated.

It has been characterized that PDCD4 can inhibit the translation of target genes through directly or indirectly binding with their mRNA (35,36). Here we have demonstrated for the first time that LXR-α is another inhibitory target of PDCD4 in high-fat circumstances, which is supported by several lines of evidence. First, HFD feeding induced repression of LXR-α protein in the adipose and the liver from WT mice and derepression in those from PDCD4$^{-/-}$ mice. Second, PA or oxLDL treatment elicited suppression of LXR-α in WT macrophages and elevation in PDCD4$^{-/-}$ macrophages. Third, RIP assay revealed the binding of PDCD4 with LXR-α mRNA in oxLDL-treated WT macrophages. These data suggest the suppression of LXR-α mediated by PDCD4 occurred most likely on posttranscriptional levels. Although the upregulation of LXR-α mRNA levels in HFD-fed PDCD4$^{-/-}$ mice can be explained by the autoregulation of LXR-α as described in previous studies (20,47), we cannot rule out the possibility of transcriptional regulation of PDCD4 on LXR-α mRNA. Interestingly, we found no increase of PDCD4 protein in HFD-fed WAT or liver, as well as oxLDL or PA-treated macrophages (Supplementary Fig. 6), but instead found the translocation of PDCD4 from nucleus to cytoplasm (data not shown), indicating PDCD4 works mainly through translocation to cytoplasm other than upregulating protein levels.

Taken together, our data demonstrate that PDCD4 deficiency protects the mice from HFD-induced obesity, WAT inflammation, insulin resistance, and fatty liver. We propose LXR-α as a new target of PDCD4 in response to HFD. PDCD4 selectively inhibits the upregulation of LXR-α in WAT and then its target genes; the suppression of these genes disturbs the homeostasis of lipid metabolism and ER function, thereby leading to obesity, WAT inflammation, and metabolic disorders (Fig. 8*I*). Although both macrophages and adipocytes link closely to the metabolic effects due to their crucial role in lipid metabolism, functions may vary in different obesity-associated diseases. Anyway, the pivotal role of PDCD4 in diet-induced obesity may add it on the list of potential targets for treating obesity-associated diseases.

ACKNOWLEDGMENTS

This study was supported partially by the National Natural Science Foundation of China (81270923, to Q.W.; 81172863, to L.Z.), the National "973" Program of China (2011CB503906, to Mei Zhang, Qilu Hospital, Shandong University, Jinan, China, with subcontract to L.Z.), the Shandong Young Scientists Award Fund (2011BSE27110, to Q.W.), and the

Independent Innovation Foundation of Shandong University (2012TS111, to Q.W.).

No potential conflicts of interest relevant to this article were reported.

Q.W., Z.D., X.L., X.S., and Q.Sh. researched data. Q.W. wrote the manuscript. Z.D. and L.Z. contributed to discussion. X.S. edited the manuscript. Q.So. Y.J., and C.G. provided technical assistance. L.Z. reviewed and edited the manuscript. Q.W. is the guarantor of this work and, as such, had full access to all the data in the study and takes responsibility for the integrity of the data and the accuracy of the data analysis.

The authors acknowledge Y.H. Chen, University of Pennsylvania School of Medicine, for providing the PDCD4$^{-/-}$ mice; F. Gao, Key Laboratory of Cardiovascular Remodeling and Function Research, Qilu Hospital, Shandong University, China, for providing 3T3-L1 cell line; and H. Wu, Baylor College of Medicine, for technical assistance, critical reading, and discussion for this study.

REFERENCES

1. Hossain P, Kawar B, El Nahas M. Obesity and diabetes in the developing world—a growing challenge. N Engl J Med 2007;356:213–215
2. Flegal KM, Carroll MD, Ogden CL, Curtin LR. Prevalence and trends in obesity among US adults, 1999-2008. JAMA 2010;303:235–241
3. Hotamisligil GS. Inflammation and metabolic disorders. Nature 2006;444:860–867
4. Xu H, Barnes GT, Yang Q, et al. Chronic inflammation in fat plays a crucial role in the development of obesity-related insulin resistance. J Clin Invest 2003;112:1821–1830
5. Mangge H, Almer G, Truschnig-Wilders M, Schmidt A, Gasser R, Fuchs D. Inflammation, adiponectin, obesity and cardiovascular risk. Curr Med Chem 2010;17:4511–4520
6. Nishimura S, Manabe I, Nagai R. Adipose tissue inflammation in obesity and metabolic syndrome. Discov Med 2009;8:55–60
7. Wu H, Ghosh S, Perrard XD, et al. T-cell accumulation and regulated on activation, normal T cell expressed and secreted upregulation in adipose tissue in obesity. Circulation 2007;115:1029–1038
8. Shibahara K, Asano M, Ishida Y, Aoki T, Koike T, Honjo T. Isolation of a novel mouse gene MA-3 that is induced upon programmed cell death. Gene 1995;166:297–301
9. Lankat-Buttgereit B, Göke R. The tumour suppressor Pdcd4: recent advances in the elucidation of function and regulation. Biol Cell 2009;101:309–317
10. Lankat-Buttgereit B, Göke R. Programmed cell death protein 4 (pdcd4): a novel target for antineoplastic therapy? Biol Cell 2003;95:515–519
11. Zhu S, Wu H, Wu F, Nie D, Sheng S, Mo YY. MicroRNA-21 targets tumor suppressor genes in invasion and metastasis. Cell Res 2008;18:350–359
12. Chen Y, Knösel T, Kristiansen G, et al. Loss of PDCD4 expression in human lung cancer correlates with tumour progression and prognosis. J Pathol 2003;200:640–646
13. Zhang H, Ozaki I, Mizuta T, et al. Involvement of programmed cell death 4 in transforming growth factor-beta1-induced apoptosis in human hepatocellular carcinoma. Oncogene 2006;25:6101–6112
14. Gao F, Zhang P, Zhou C, et al. Frequent loss of PDCD4 expression in human glioma: possible role in the tumorigenesis of glioma. Oncol Rep 2007;17:123–128
15. Wei ZT, Zhang X, Wang XY, et al. PDCD4 inhibits the malignant phenotype of ovarian cancer cells. Cancer Sci 2009;100:1408–1413
16. Sheedy FJ, Palsson-McDermott E, Hennessy EJ, et al. Negative regulation of TLR4 via targeting of the proinflammatory tumor suppressor PDCD4 by the microRNA miR-21. Nat Immunol 2010;11:141–147
17. Ruan Q, Wang T, Kameswaran V, et al. The microRNA-21-PDCD4 axis prevents type 1 diabetes by blocking pancreatic beta cell death. Proc Natl Acad Sci USA 2011;108:12030–12035
18. Apfel R, Benbrook D, Lernhardt E, Ortiz MA, Salbert G, Pfahl M. A novel orphan receptor specific for a subset of thyroid hormone-responsive elements and its interaction with the retinoid/thyroid hormone receptor subfamily. Mol Cell Biol 1994;14:7025–7035
19. Auboeuf D, Rieusset J, Fajas L, et al. Tissue distribution and quantification of the expression of mRNAs of peroxisome proliferator-activated receptors and liver X receptor-alpha in humans: no alteration in adipose tissue of obese and NIDDM patients. Diabetes 1997;46:1319–1327
20. Wójcicka G, Jamroz-Wiśniewska A, Horoszewicz K, Bełtowski J. Liver X receptors (LXRs). Part I: structure, function, regulation of activity, and role in lipid metabolism. Postepy Hig Med Dosw (Online) 2007;61:736–759
21. Ducheix S, Lobaccaro JM, Martin PG, Guillou H, Liver X. Liver X receptor: an oxysterol sensor and a major player in the control of lipogenesis. Chem Phys Lipids 2011;164:500–514
22. Oosterveer MH, Grefhorst A, Groen AK, Kuipers F. The liver X receptor: control of cellular lipid homeostasis and beyond Implications for drug design. Prog Lipid Res 2010;49:343–352
23. Calkin AC, Tontonoz P. Transcriptional integration of metabolism by the nuclear sterol-activated receptors LXR and FXR. Nat Rev Mol Cell Biol 2012;13:213–224
24. Fu S, Yang L, Li P, et al. Aberrant lipid metabolism disrupts calcium homeostasis causing liver endoplasmic reticulum stress in obesity. Nature 2011;473:528–531
25. Gregor MF, Hotamisligil GS. Thematic review series: Adipocyte Biology. Adipocyte stress: the endoplasmic reticulum and metabolic disease. J Lipid Res 2007;48:1905–1914
26. Erbay E, Babaev VR, Mayers JR, et al. Reducing endoplasmic reticulum stress through a macrophage lipid chaperone alleviates atherosclerosis. Nat Med 2009;15:1383–1391
27. Soccio RE, Adams RM, Maxwell KN, Breslow JL. Differential gene regulation of StarD4 and StarD5 cholesterol transfer proteins. Activation of StarD4 by sterol regulatory element-binding protein-2 and StarD5 by endoplasmic reticulum stress. J Biol Chem 2005;280:19410–19418
28. Gao Q, Jiang Y, Ma T, et al. A critical function of Th17 proinflammatory cells in the development of atherosclerotic plaque in mice. J Immunol 2010;185:5820–5827
29. Liu XL, Zhang PF, Ding SF, et al. Local gene silencing of monocyte chemoattractant protein-1 prevents vulnerable plaque disruption in apolipoprotein E-knockout mice. PLoS ONE 2012;7:e33497
30. Hotamisligil GS. Endoplasmic reticulum stress and inflammation in obesity and type 2 diabetes. Novartis Found Symp 2007;286:86–94; discussion 94–88, 162–163, 196–203
31. Hummasti S, Hotamisligil GS. Endoplasmic reticulum stress and inflammation in obesity and diabetes. Circ Res 2010;107:579–591
32. Boden G, Duan X, Homko C, et al. Increase in endoplasmic reticulum stress-related proteins and genes in adipose tissue of obese, insulin-resistant individuals. Diabetes 2008;57:2438–2444
33. Boden G, Merali S. Measurement of the increase in endoplasmic reticulum stress-related proteins and genes in adipose tissue of obese, insulin-resistant individuals. Methods Enzymol 2011;489:67–82
34. Ozcan U, Cao Q, Yilmaz E, et al. Endoplasmic reticulum stress links obesity, insulin action, and type 2 diabetes. Science 2004;306:457–461
35. Singh P, Wedeken L, Waters LC, Carr MD, Klempnauer KH. Pdcd4 directly binds the coding region of c-myb mRNA and suppresses its translation. Oncogene 2011;30:4864–4873
36. Wedeken L, Singh P, Klempnauer KH. Tumor suppressor protein Pdcd4 inhibits translation of p53 mRNA. J Biol Chem 2011;286:42855–42862
37. Hotamisligil GS. Inflammation and endoplasmic reticulum stress in obesity and diabetes. Int J Obes (Lond) 2008;32(Suppl. 7):S52–S54
38. Hotamisligil GS. Endoplasmic reticulum stress and the inflammatory basis of metabolic disease. Cell 2010;140:900–917
39. Awazawa M, Ueki K, Inabe K, et al. Adiponectin suppresses hepatic SREBP1c expression in an AdipoR1/LKB1/AMPK dependent pathway. Biochem Biophys Res Commun 2009;382:51–56
40. Sampath H, Ntambi JM. Polyunsaturated fatty acid regulation of gene expression. Nutr Rev 2004;62:333–339
41. Brown MS, Goldstein JL. Selective versus total insulin resistance: a pathogenic paradox. Cell Metab 2008;7:95–96
42. Shimomura I, Matsuda M, Hammer RE, Bashmakov Y, Brown MS, Goldstein JL. Decreased IRS-2 and increased SREBP-1c lead to mixed insulin resistance and sensitivity in livers of lipodystrophic and ob/ob mice. Mol Cell 2000;6:77–86
43. Laurencikiene J, Rydén M. Liver X receptors and fat cell metabolism. Int J Obes (Lond) 2012;36:1494–1502
44. Gao M, Liu D. The liver X receptor agonist T0901317 protects mice from high fat diet-induced obesity and insulin resistance. AAPS J 2013;15:258–266
45. Dong B, Kan CF, Singh AB, Liu J. High-fructose diet downregulates long-chain acyl-CoA synthetase 3 expression in liver of hamsters via impairing LXR/RXR signaling pathway. J Lipid Res 2013;54:1241–1254
46. Korach-André M, Archer A, Gabbi C, et al. Liver X receptors regulate de novo lipogenesis in a tissue-specific manner in C57BL/6 female mice. Am J Physiol Endocrinol Metab 2011;301:E210–E222
47. Li Y, Bolten C, Bhat BG, et al. Induction of human liver X receptor alpha gene expression via an autoregulatory loop mechanism. Mol Endocrinol 2002;16:506–514